PRAMANA
— journal of
physics

Vol. 59, No. 1
July 2002
pp. L155–L161

Fractal patterns on the onset of coherent structures in a coupled map lattice

G AMBIKA and KAMALA MENON
Department of Physics, Maharaja's College, Cochin 682 011, India

MS received 14 February 2002

Abstract. We report the formation of Cantor set-like fractals during the development of coherent structures in a coupled map lattice (CML). The dependence of these structures on the size of the lattice as well as the first three dimensions of the associated fractal patterns are analyzed numerically.

Keywords. Fractal dimensions; coherent structures; coupled map lattice.

PACS Nos 05.45.Ra; 05.45.-a; 05.45.Jn; 05.45.Ac; 05.45.Xt

A coupled map lattice (CML) is a mathematical representation of a high-dimensional non-linear system in which space and time are discrete but state variables are continuous. This discreteness makes their simulation easier than continuous spatiotemporal systems like turbulent fluids and hence CML has served as an ideal candidate in the study of spatiotemporal complexity in general [1–8]. They also model pattern formation and evolution in spatially extended systems like chemical diffusion reactions [9,10], a variety of biological systems [11] and population dynamics [12,13]. Most of the dynamical properties of CML have been explored extensively during the past decade [6,14–16] like high-dimensional chaos including spatiotemporal intermittency, control of spatiotemporal chaos [17] and synchronization [18,19]. Recent works on CML deal with many specific and novel features like multiplicative diffusion [20], traveling fronts [21], synchronization [22–24], bubble cascades [25], asynchronous updating [26] etc.

The basic structure of a CML consists of a local dynamics modeled by a non-linear transformation of the variable given by non-linear maps. These are arranged on a lattice and the coupling among them can be suitably chosen as nearest neighbor with periodic boundary conditions, one way coupling or global coupling. Simple one-dimensional models of this type are usually expressed as

$$x_{n+1}(i) = \alpha f(x_{n+1}(i)) + \beta g[f(x_n(i), f(x_n(i+1), f(x_n(i-1)] \tag{1}$$

where the function g governs the nature of the coupling. If

$$g = f(x_n(i+1)) + f(x_n(i-1)) - 2f(x_n(i)) \tag{2}$$

it is diffusive coupling, and if

$$g = f(x_n(i)) - f(x_n(i-1)) \tag{3}$$

it is one way coupling [27], and if

$$g = \sum_{j=1}^{N} f(x_n(j)) \tag{4}$$

it is global coupling [22,24,28] etc.

α and β are parameters that take care of non-linearity and coupling strengths. The map for local dynamics is $f(x_n(i))$ with n representing the temporal iteration index and i and j refer to the lattice sites.

Here in our work, the on-site map is the usual logistic map and we concentrate mainly on symmetric diffusive coupling with nearest neighbors and periodic boundary conditions. The strength of the coupling is expressed through a parameter ε, so that the system under present study is

$$x_{n+1}(i) = (1-\varepsilon) f(x_n(i)) + \frac{\varepsilon}{2}(f(x_n(i+1) + f(x_n(i-1)) \tag{5}$$

with

$$f(x_{n+1}(i)) = \mu x_n(i)(1 - x_n(i)) \tag{6}$$

and

$$x_n(L+1) = x_n(1) \tag{7}$$

where L is the size of the lattice measured by the total number of lattice sites included in the calculation. The standard time evolution is employed by parallel or synchronous updating where all individual maps are iterated forward simultaneously. The value of the parameter μ in our studies is the accumulation point or Feigenbaum point, viz., $\mu_\alpha = 3.569944$, where the first transition to chaos takes place in the uncoupled case. It is an established result [29] that due to coupling each site can be taken through a reverse period doubling sequence to one-cycle again as ε is slowly tuned. Then it is possible to locate regions where synchronized spatiotemporal fixed point has stability. This leads the lattice to a coherent mode asymptotically. Earlier studies in the occurrence of such coherent modes are mainly in the periodic regime of the local dynamics. Thus for μ corresponding to periodic regions ($\mu < 3$), total coherence has been observed independent of the lattice size [17]. By fixing ε at 0.9, we ensure the possibility of coherent structure formation along the lattice. Our analysis indicates that for $\mu = \mu_\infty$, very small lattices become synchronous spatially and have totally coherent frozen structures asymptotically. However, as the lattice size increases, such a structure loses stability and slowly evolves again to total coherence as L is increased. During this process, we recognize fractal patterns that belong to non-uniform Cantor sets on the lattice background. They are geometrically characterized by calculating the first three dimensions, viz., D_0, D_1 and D_2 using a modified box counting algorithm. The finite size effects and identification and characterization of coherent structures are the main results reported in this letter.

For the parameter values chosen ($\mu = \mu_\infty = 3.569944$ and $\varepsilon = 0.9$), simultaneous updating is done at all lattice sites by iterating each map 11000 times. The asymptotic values

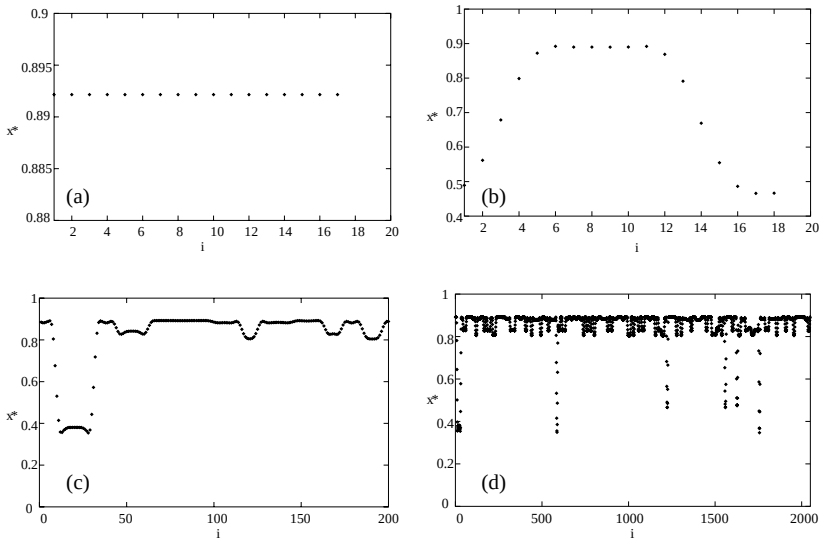

Figure 1. The asymptotic values of x^* at each site plotted against site number i. (**a**) $L = 17$; (**b**) $L = 18$; (**c**) $L = 200$ and (**d**) $L = 2048$. The sudden departure from complete coherence at $L = 18$ and the increasing tendency to settle to coherence and the development of coherent structures of finite size, as L increases, are clearly visible.

Table 1. The decoherence parameter γ calculated for increasing values of L, $n = 11000$.

L	γ
16	0
32	0.284679
64	0.327383
128	0.210977
256	0.252978
512	0.109721
1024	0.088239
2048	0.083201
4096	0.080306
8192	0.075644

are checked for coherence. It is found that for small values of L say up to $L = 17$, the system settles down to complete coherence with an x value, $x^* = 0.89$ (figure 1a). This coherence is lost at $L = 18$ (figure 1b) and there after the system never settles to complete coherence even for large values of n, although there is an increasing tendency for that as L is increased. However up to $L = 200$, there is no particular pattern (figure 1c) and above 200, coherent structures of finite size develop (figure 1d) with $x^* = 0.89 \pm 0.003$.

To quantify this tendency and index it properly we define a decoherence parameter γ as the mean square deviation from x^*. This is computed for values of L from 16 to 8192 and presented in table 1. Figure 2 gives a plot of these values up to $L = 8192$. The value of γ is zero up to $L = 17$ and at $L = 18$, there is a steep rise in the value which falls slowly as L is increased, indicating an increase in the tendency for coherent structure formation.

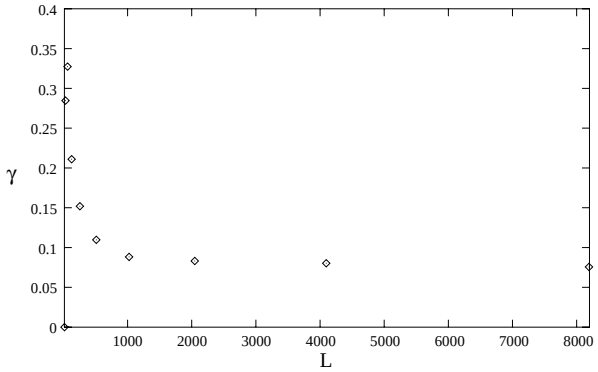

Figure 2. Variation of the decoherence parameter γ with the lattice size L. The onset of decoherence after $L = 17$ and its further decrease with increasing L are clear.

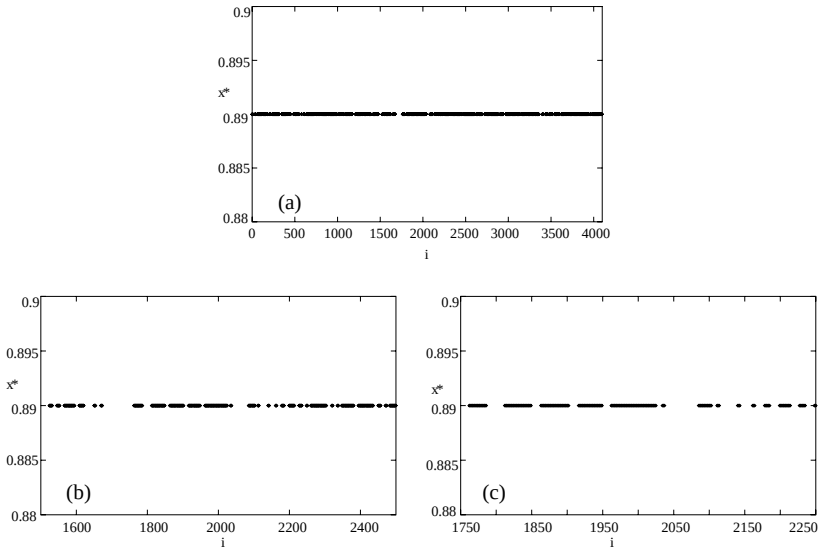

Figure 3. Asymptotic values of $x_n(i)$ viz. x^* plotted against site number for $L = 4096$. The Cantor-like fractal geometry is visible. The finer and finer structures can be brought out by zooming into different regions. (**a**) The fractal set for the full lattice. (**b**) The sublattice ($i = 1500$–2500) and (**c**) is for the sublattice ($i = 1750$–2250).

It is to be noted that even though γ decreases with increasing L, total coherence is not achieved even for large L and large n (11000). Hence if we plot x^* as a function of the lattice site ($L > 200$), coherent structures are locally finite in length with gaps in between, resembling a non-uniform Cantor set. Here the plotted x values are not the iterates in time but the asymptotic value at each site and hence the geometry of the resulting Cantor-like fractal is set on the discrete lattice background (figure 3). To characterize its dimensions, we follow a box counting procedure that is a slight variant of the usual procedure, neces-

sitated by the discreteness of the lattice. It is clear that the box size cannot be reduced to limit zero, the minimum being set by one lattice site. As the first step, one half of the lattice size, viz. $L/2$, is taken as the box size, r, and $N(r)$ is counted. In the second step, $r = L/4$ and the process is repeated until $r = 1$. It has been observed that in the limiting case of $r = 1$, the three dimensions D_0, D_1 and D_2 are equal, as is expected similar to the limiting case of $\varepsilon = 0$ in the continuous case. Also we find $D_0 > D_1 > D_2$, same as in the continuous case. For convenience, in L only powers of 2 are considered. However, we have checked the values by considering other values for L also.

The values of D_0, D_1 and D_2 for $L = 8192$ and different r values are shown in table 2. The $\ln(N(r))$ vs. $\ln(1/r)$ for D_0 with $L < 200$ (figure 4a) shows no noticeable average shape. However for $256 < L < 300$ (figure 4c) there is a tendency towards a straight line behavior with uniform slope and for $L > 300$ (figure 4e), the straight line portion is predominant. This is reflected in the slopes of these graphs, i.e., D_0 values plotted against the size of the lattice (figures 4b, 4d, 4f).

Table 2. The values of D_0, D_1 and D_2 calculated for different box sizes, and $L = 8192$, $n = 11000$.

Box size r	D_0	D_1	D_2
1	0.892301	0.892301	0.892301
2	0.894064	0.891112	0.889078
4	0.906111	0.893981	0.887154
8	0.933316	0.903142	0.887846
16	0.97461	0.922824	0.896236
32	0.995	0.944831	0.919396
64	1	0.964933	0.943931
128	1	0.983164	0.970162

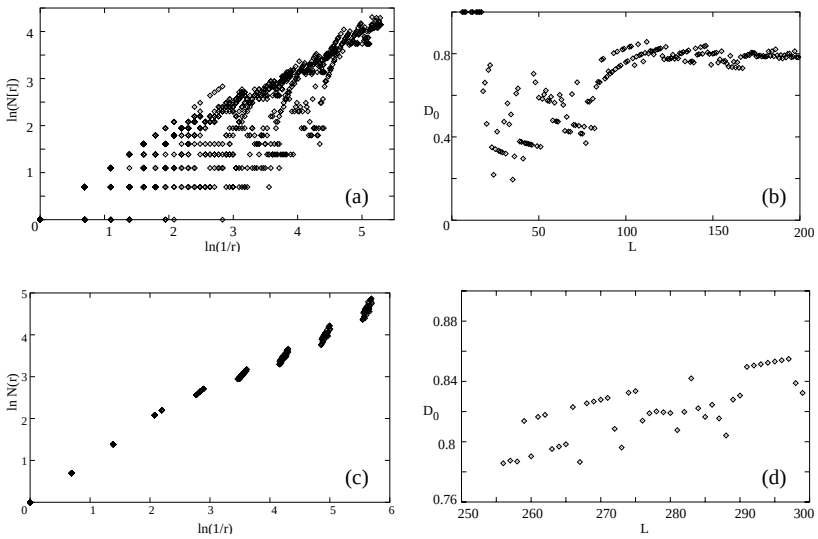

Figure 4(a)–(d).

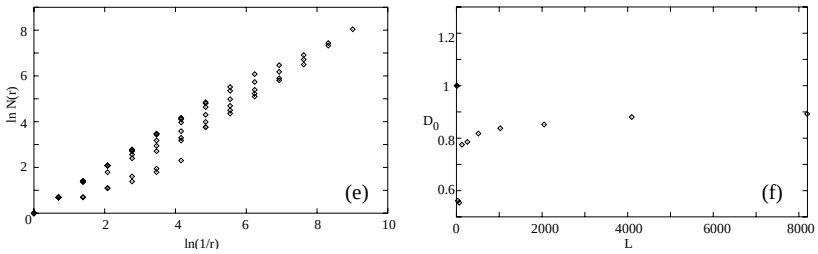

Figure 4. The $\ln(N(r))$ vs. $\ln(1/r)$ graphs (a, c, e) and the corresponding slopes for D_0 vs. size of the lattice (b, d, f) for different lattice sizes. (**a**), (**b**) For $L < 200$, (**c**), (**d**) for $256 < L < 300$ and (**e**), (**f**) for $L > 300$.

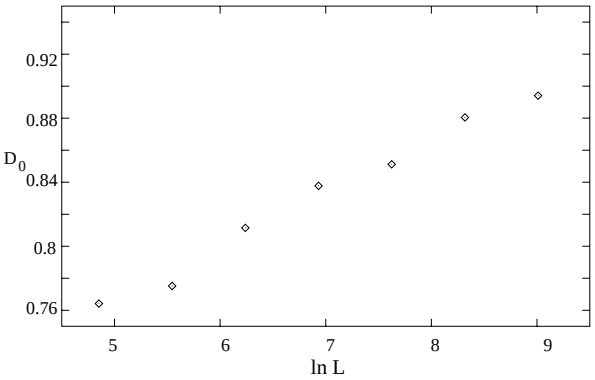

Figure 5. A plot of D_0 against $\ln(L)$.

It is clear that below 200, D_0 values are scattered but as L increases, D_0 increases rapidly with L. From the plot of D_0 vs. L (figure 4f), it is clear that this increase can be modeled by an exponential relationship of the form

$$L \propto \mathrm{e}^{bD_0}$$

where b is a parameter that may in general depend on μ and ε. In figure 5, we plot the value of D_0 for $r = 2$ against $\ln(L)$. The resulting straight line has an average slope from which $b = 52.63$.

In conclusion, we have numerically analyzed the effect of finite size of the lattice in the formation of coherent structures in a CML. We report that during the development of these structures with increasing lattice size, Cantor-like fractals can be visualized. The dimensions characterizing them are studied for different L and D_0 and found to depend logarithmically on L. The calculations are repeated by changing ε and the behavior qualitatively remains the same. Further work directed towards analysis of sites that fall in the gaps of the Cantor-like set and the onset of synchronicity at sites that belong to the set are in progress and will be reported elsewhere.

References

[1] A R Bishop, G Gruner and B Nicolaenko (eds) *Physica* **D23** (1986)
[2] K Kaneko, *Physica* **D41**, 137 (1990)
[3] G Perez, S Sinha and H A Cerdeira, *Physica* **D63**, 341 (1993)
[4] K Kaneko, *Theory and applications of coupled map lattices* (Wiley, NY, 1993)
[5] C Beck, *Phys. Rev.* **E49**, 3641 (1994)
[6] K Kaneko, *Physica* **D37**, 60 (1989)
[7] Y Yanagita and K Kaneko, *Phys. Lett.* **A175**, 415 (1993)
[8] F H Willeboordse and K Kaneko, *Physica* **D86**, 428 (1995)
[9] G Veser, F Mertens, A S Mikhailov and R Imbihl, *Phys. Rev. Lett.* **71**, 935 (1993)
[10] R Kapral, R Livi, G L Oppo and A Politi, *Phys. Rev.* **E49**, 2009 (1994)
[11] H Meinhardt, *Models of biological pattern formation* (Academic, NY, 1982)
[12] M P Hassell, O Miramontes, P Rohani and R M May, *J Animal Eco.* **64**, 662 (1995)
[13] R V Sole and J Bascompte, *J. Theor. Biol.* **175**, 139 (1995)
[14] K Kaneko, *Physica* **D55**, 368 (1992)
[15] K Kaneko, *Physica* **D54**, 5 (1992)
[16] K Ikede, K Otsuka and K Matsumoto, *Prog. Theor. Phys. Suppl.* **99**, 195 (1989)
[17] P Parmananda and Yu Jiang, *Phys. Lett.* **A231**, 159 (1997)
[18] S Parthasarathy and J Gue'mez, *Ecological modelling* **106**, 17 (1998)
[19] F S de San Roman, S Boccalatti, D Maza and H Mancini, *Phys. Rev. Lett.* **81**, 3639 (1998)
[20] W Wang and H A Cerdeira, *Chaos* **6(2)**, 200 (1996)
[21] R C Gonzalez, D K Arrowsmith and F Vivaldi, *Phys. Rev.* **E61**, 1329 (2000)
[22] M Mehta and S Sinha, *Chaos* **10**, 350 (2000)
[23] M B Ouchi and K Kaneko, *Chaos* **10**, 350 (2000)
[24] Paul Glendinning, *Phys. Lett.* **A259**, 129 (1999)
[25] Noriyuki Bob Ouchi and Kunihiko Kaneko, *Chaos* **10**, 359 (2000)
[26] Mitaxi Mehta and Sudeshna Sinha, *Chaos* **10**, 350 (2000)
[27] Keiji Konishi, Hideki Kokame and Kentaro Hirata, *Phys. Lett.* **A263**, 307 (1999)
[28] Yu Jiang, A Antillon and J Escalona, *Phys. Lett.* **A262**, 403 (1999)
[29] R E Amritkar and P M Gada, *Phys. Rev. Lett.* **70**, 1408 (1993)